Available online at www.sciencedirect.com
SCIENCE DIRECT®
International Journal of Heat and Mass Transfer 47 (2004) 1965–1977
International Journal of HEAT and MASS TRANSFER
www.elsevier.com/locate/ijhmt

Study on propagative collapse of a vapor film in film boiling (mechanism of vapor-film collapse at wall temperature above the thermodynamic limit of liquid superheat)

Hiroyasu Ohtake *, Yasuo Koizumi

Department of Mechanical Engineering, Kogakuin University, 2665-1, Nakano-machi, Hachioji-shi, Tokyo 192-0015, Japan

Received 5 December 2002; received in revised form 1 September 2003

Abstract

This paper investigates the mechanism of vapor-film collapse by a propagative collapse for film boiling at high wall-superheat. It also reports effects of a local-cold spot on both the minimum-heat-flux (MHF) temperature and the way in which the vapor film would collapse. Experimental results showed that propagation velocity of vapor-film collapse would decrease and MHF temperature would increase when the local-cold spot temperature was decreased. The results also showed that the MHF temperature increased remarkably when the local-cold spot temperature was lower than the thermodynamic limit of liquid superheat, T_{tls}. It was proved through analytical and numerical models that local temperature at the collapse front of the vapor film, namely the local solid surface temperature at the position of liquid–solid contact, could never exceed the T_{tls} even if the vapor-film collapse occurred at a high wall-superheat.

Keywords: Boiling heat transfer; Minimum heat flux; Thermodynamic limit of liquid superheat

1. Introduction

When a hot metal object is submerged in a liquid, film boiling will take place at first. At a later stage, however, the liquid will make substantial contact with the metal surface at a certain condition. Subsequently, the vapor film of the film boiling will collapse onto the metal surface. The collapse of the vapor film has traditionally been related to the minimum-heat-flux-point (MHF-point) of a boiling curve, as found by Nukiyama [1] in 1943. It has also been used to describe a number of phenomena such as the Leidenfrost, quenching and rewetting phenomena. It is of extreme importance to understand the collapse conditions in some industrial situations. Examples are: assessing the reliability of the emergent core cooling system (ECCS) in the case of loss-of-coolant accidents (LOCAs) of light-water-reactors (LWRs), analyzing thermal stability of superconducting magnets and controlling the metallurgical structure in manufacturing steel.

Many attempts have been made by several investigators to examine the mechanism of the vapor-film collapse in the film boiling or in other words, the MHF condition. For example, in an early work, Berenson [2] analyzed the MHF heat flux q_{MHF} based on the heat-flux-controlled hypothesis and reported the following correlation:

$$q_{MHF} = 0.09\rho_v h_{fg}\left[\frac{g(\rho_l-\rho_v)}{\rho_l+\rho_v}\right]^{1/2}\left[\frac{\sigma}{g(\rho_l-\rho_v)}\right]^{1/4}, \quad (1)$$

where σ is surface tension and g is acceleration of gravity. Recently, Nishio [3] reported the following correlation for the MHF-point temperature T_{MHF} of saturated water at atmospheric pressure based on the temperature-controlled hypothesis:

* Corresponding author. Tel.: +81-426-28-4172; fax: +81-426-27-2360.
E-mail address: ohtake@cc.kogakuin.ac.jp (H. Ohtake).

0017-9310/$ - see front matter © 2003 Elsevier Ltd. All rights reserved.
doi:10.1016/j.ijheatmasstransfer.2003.09.020

Nomenclature

c	specific heat
D	diameter of heated wire
h_{fg}	latent heat
I	supply current
k	thermal conductivity
q_w	wall heat flux
r, R	radius
T_0	temperature of film-boiling vapor-layer's collapse front
T_{elc}	electrode temperature (local temperature of low-temperature section)
T_{MHF}	minimum-heat-flux-point temperature (average boiling surface temperature when vapor-layer collapses)
T_{sat}	saturation temperature
T_{shn}	spontaneous homogenous nucleation temperature
T_{tls}	thermodynamic limit of liquid superheat
T_{wi}	maximum permissible liquid–solid contact-temperature based on two-body contact model
ΔT_{sat}	degree of superheat ($= T_w - T_{sat}$)
ΔT_{sub}	degree of liquid subcooling ($= T_{sat} - T_l$)
w	propagation velocity of collapse of film-boiling vapor film
ρ	density
ρ_e	electrical resistively

Subscripts

l	liquid
v	vapor
w	wall

$$T_{MHF} = 200\ ^\circ\mathrm{C}. \tag{2}$$

However, this temperature is sensitive to the characteristics of the boiling surface, and as a result, it is very rare that the above temperature is achieved in industrial situations. Especially, this tendency is marked in the case of subcooled boiling, in which case the MHF temperature is known to be described by the following empirical equation by Dhir and Purohit [4]:

$$T_{MHF} = 201 + 8\Delta T_{sub}\ ^\circ\mathrm{C}. \tag{3}$$

Contrarily, it is also reported by Narasaki et al. [5] that a careful preparation of the boiling surface will result in $\Delta T_{MHF} = 200\ ^\circ\mathrm{C}$ even at $\Delta T_{sub} = 80$ K; this makes it clear that MHF-point temperature can vary drastically depending on the researcher and the apparatus being used. In addition, the above equation predicts values that exceed the thermodynamic limit of liquid superheat (T_{tls}) for subcoolings larger than $\Delta T_{sub} = 14$ K; for water at one atmosphere, $T_{tls} = 310\ ^\circ\mathrm{C}$ roughly. Therefore, the possibility of seeking a physical interpretation to the above equation seems doubtful.

The causes for such discrepancies are attributed mainly to the existence of localized low-temperature spots (or weak spots) on the boiling surface and to different ways in which the film-boiling vapor layer can collapse starting from the weak spots, as pointed out by Nishio et al. [6]. One such way of collapse is the collapse that starts from a localized low-temperature spot, spreading to the entire boiling surface. Following Ref. [6], we call this type of collapse a propagative vapor-layer collapse. In this type, the MHF point will appear to have been elevated to a higher temperature because the vapor-collapse results from a localized low-temperature spot. In addition, in this type of collapse, a large temperature gradient will occur within the boiling surface, and therefore, heat conduction within the boiling surface will be a governing factor of the collapse phenomenon.

Another type of collapse is the collapse of the vapor layer simultaneously and uniformly over the boiling surface; this collapse is referred to as a coherent collapse following Ref. [6]. In this type, the boiling surface has a uniform temperature, and the temperature at the collapse can possibly be determined by considering hydrodynamics of the vapor layer of film boiling. In general, this collapse method is observed under laboratory conditions, but in industrial situations, the former method of collapse is more common.

The two types of collapse mechanisms mentioned above have also been reported by Kikuchi et al. [7] (using a spherical surface) and Narazaki et al. [5] (using a vertical cylindrical surface). Although they have done a qualitative assessment of the phenomenon, so far a quantitative assessment has not been performed. For the same reason, a physical interpretation has not been proposed as to why the MHF-point temperature in reality exceeds the thermodynamic limit of liquid superheat.

In the present work, we have experimentally examined the above issue, namely the issue of the difference and relationship between the MHF-point temperatures under idealized conditions of laboratory and under industrial situations; to do that, we focused on the method of collapse of film-boiling vapor layer and on the temperature of low-temperature section. Then, we proposed a solution to the issue of why MHF-point temperature in reality exceeds the thermodynamic superheat

limit by using our experimental results and the results of a model analysis that was based on heat conduction.

2. Experimental apparatus and procedure

Fig. 1 shows the schematic diagram of the experimental apparatus. The boiling surface was a (99.95% pure) fine platinum wire of 1 mm diameter and 160 mm long (140 mm effective length), which was directly heated by passing a direct current through it using a stabilized DC power supply. The platinum wire was connected at each end to a silver electrode, part of which had a cartridge-type heater inserted in it to control its temperature. This set-up made it possible to avoid quite ordinary weak spots and to control freely the temperature of low-temperature sections present at each end of the wire. In addition, the middle section of the platinum wire had 3–5 voltage taps of ultra-fine platinum wires (each 30 μm in diameter) spot-welded to it at an interval of 20 mm; in this manner, we minimized the effects of weak spots at the central section of the platinum wire. Average temperature and heat flux for the platinum wire between any two adjacent voltage taps were found from temperature dependence of electrical resistance of the platinum wire by Japanese Industrial Standard [8] and Joule heat generation respectively. Experiments were conducted in a double-wall glass vessel (having 300 mm × 200 mm lengths and 200 mm height for inner bath), which was exposed to atmosphere.

The steady-state experiments were done in the following manner. First, the end-temperature of each electrode was maintained slightly above the desired temperature of the electrode. Then, after electrically heating the wire to red-hot state (roughly to a temperature of 1200 °C) in a vapor mist environment, the experimental vessel was filled with degassed and deionized water maintained at saturation temperature. With the above preparations, we establish around the platinum wire a film-boiling state in which the initial degree of superheat was 500 K. We measured film-boiling heat transfer rates when we have confirmed the stability of the temperatures of the boiling surface, electrodes, and the test liquid. To measure heat transfer rates, it was necessary to control the boiling surface temperature, power supplied to the electrodes at the two ends of the wire, power supply to the heater that controls test-liquid temperature and the liquid flow rate in the cooling line. Next, while maintaining the electrode and liquid-bath temperatures constant, we destabilized the film boiling at different temperatures by reducing the current supply to the wire step by step. The MHF point was defined by the temperature and heat flux at the instance when the vapor-film collapses. Behavior of the vapor-film during its collapse was recorded by a video camera (at 30 frames/s). The rate of vapor-film collapse was measured after the experiment by playback of the video. In addition, for the purpose of reference, voltage difference in each of the wire-segments between the platinum-wire voltage-taps was fed into a computer through an A/D converter.

In this series of experiments, we changed the electrode temperature in the range 450–250 °C, and examined the dependence of the temperature of the localized

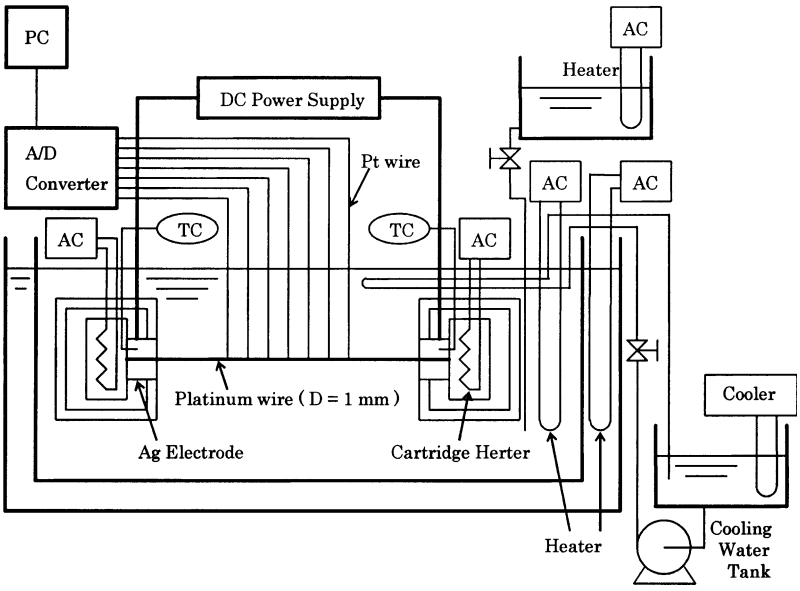

Fig. 1. Experimental apparatus.

low-temperature region on the process of vapor-film collapse (namely, on the way of collapse, the temperature and the velocity of collapse). When the vapor-layer collapses from the central section, it may be possible that the electrode temperature becomes higher than the average temperature of boiling surface. However, in the present work, the two end-electrodes were intended to become weak spots that caused the vapor-film to collapse, and the temperature of the electrodes were referred to as the localized low temperature. In the present experiment, we used the following three degrees of liquid subcoolings ΔT_{sub}: 0 K (saturated), 10 K and 20 K.

2.1. Experimental uncertainly

The platinum wire of 99.95% purity itself was used as the temperature sensor. For each section of test wire between the voltage taps, the uncertainty of its average temperature was estimated to be about ±5% (about 8 K for 250 °C), based on uncertainty of 0.05% in the voltmeter with 10 μV resolution. The difference between the wall temperature of the heating wire and the measured average temperature was estimated to be less than 1 °C based on a heat conduction analysis of a cylinder of 1 mm diameter. The temperature of the silver electrode was measured by a thermocouple fitted inside the electrode at a position about 10 mm from the surface. The temperature gradient in the silver block was moderate, because the electrode was maintained film-boiling state on its surface and silver has high heat conductivity. Thus, the difference between the measured and calculated values of the wall-temperature of the electrode was found to be less than 1 °C.

The propagation velocities of vapor-film collapse were measured on a normal monitor with a normal video tape recorder at 30 frames/s. The camera system for the observations magnified the test wire and the vapor film about twice on the monitor. The uncertainty in the propagation velocity was estimated to be about ±5% (±1.2 mm/s) for a typical propagation velocity of 30 mm/s based on a displacement of 2 mm per frame on the monitor. The maximum velocity obtained by the present data process procedure was about 1000 mm/s.

2.2. Effect of weak spots on boiling heat transfer

In order to estimate an effect of weak spots on boiling heat transfer, we calculate transient heat conduction in a finite cylinder three-dimensionally by using the following equation:

$$\frac{T^{n+1}_{i,j,k}-T^{n}_{i,j,k}}{\Delta t}=a\left\{\frac{T^{n}_{i+1,j,k}-2T^{n}_{i,j,k}+T^{n}_{i-1,j,k}}{\Delta x^2}+\frac{T^{n}_{i,j+1,k}-2T^{n}_{i,j,k}+T^{n}_{i,j-1,k}}{\Delta r^2}+\frac{1}{R_j}\frac{T^{n}_{i,j+1,k}-T^{n}_{i,j-1,k}}{2\Delta r}+\frac{1}{R_j^2}\frac{T^{n}_{i,j,k+1}-2T^{n}_{i,j,k}+T^{n}_{i,j,k-1}}{\Delta\theta^2}\right\}+\frac{\dot{q}_{\mathrm{Joule}}}{\rho c}. \tag{4}$$

Here, a is thermal diffusivity and $\dot{q}_{\mathrm{Joule}}$ is Joule heat generation rate per unit volume. As the boundary condition of the weak spot, we have made a mesh on the outside at the center of the cylinder a welding spot between a voltage tap and the cylinder by assigning the welding spot calculated value on heat conduction through the voltage tap:

$$q_{\text{voltage tap}}=k_{\mathrm{w}}(T_{\mathrm{w}}-T_{\mathrm{sat}})/\delta_{\mathrm{v}}=k_{\mathrm{w}}\Delta T_{\mathrm{sat}}/(k_{\mathrm{v}}/h_{\mathrm{f}})=(k_{\mathrm{w}}/k_{\mathrm{v}})q_{\mathrm{w}}. \tag{5}$$

Here δ_{v} is a thickness of vapor film of film boiling: the value is estimated at $k_{\mathrm{v}}/h_{\mathrm{f}}$.

In Fig. 2, we show temperature distributions on r–θ cross section and r–z cross section by the present calculation for the case of the wall temperature $T_{\mathrm{w}}=300$ °C and 30 μm in diameter of the voltage tap. As seen from Fig. 2, the temperature drop at just the welding

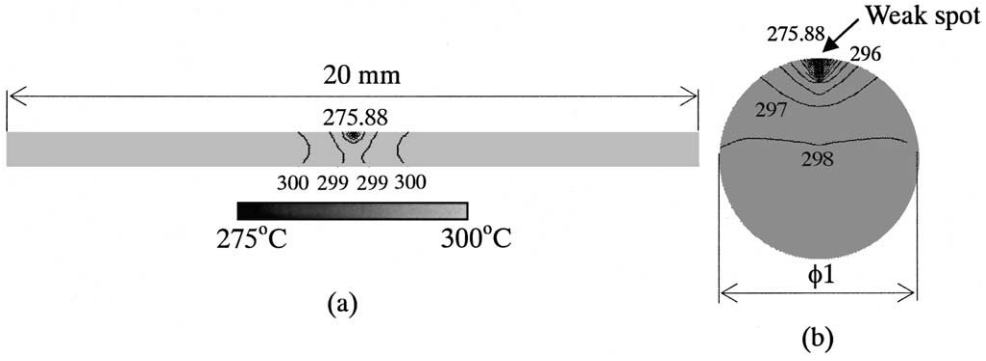

Fig. 2. Temperature distributions on (a)r–z and (b) r–θ cross sections.

spot is about 25 °C for the case of $T_w = 300$ °C and saturated condition. Namely, the temperature drop at the welding spot is estimated to be 8.5% in film-boiling regime. The heat loss rate through the weak spot is 0.205 W/s, the quantity is much smaller than heat transfer rate on a overall wall between voltage taps, 4.67 W/s. The calculated result for the case of the wall temperature $T_w = 600$ °C is similar to that for the case of $T_w = 300$ °C.

3. Experimental results and discussion

3.1. Saturated boiling

Fig. 3 is a saturated boiling curve representing the relationship between the wall heat flux q_w and wall-superheat ΔT_{sat} for the case of the electrode temperature $T_{elc} = 450$ °C; the parameter of the figure is the axial position along the boiling surface. The figure also shows the following relationships: equations of Rohsenow [9] for nucleate boiling heat flux q_{nb}, Lienhard and Dhir [10] for critical heat flux q_{CHF} in the case of a fine horizontal wire and Baumeister and Hamill [11] for coefficient of film-boiling heat transfer h_f, and the relationship of Nishio [3] for MHF-point temperature as given by Eq. (2). The numbers in the legend of Fig. 3 are the distances from the right electrode to the middle of a measurement segment of wire between a pair of platinum-wire voltage-taps. As seen from Fig. 3, film-boiling heat transfer coefficient is independent of the position on the heat transfer surface at steady-state boiling, and is in agreement with the known relationships. In addition, the MHF-point temperature, which is the average heat transfer surface temperature when the vapor-film collapses, also agrees with the existing relationships, 200 °C. Even at other electrode temperatures, the film-boiling heat transfer coefficient at steady state was independent of the position on the heat transfer surface and was in agreement with existing relationships. The effects of electrode temperature, which is the temperature of localized low-temperature region, on the boiling curve are shown in Fig. 4. From this figure, it is clear that the MHF-point temperature moves to higher values when the electrode temperature decreases. Especially, this tendency is drastic when the electrode temperature is below 300 °C.

The MHF-point temperatures obtained in the present series of experiments were shown in Fig. 5 as a function

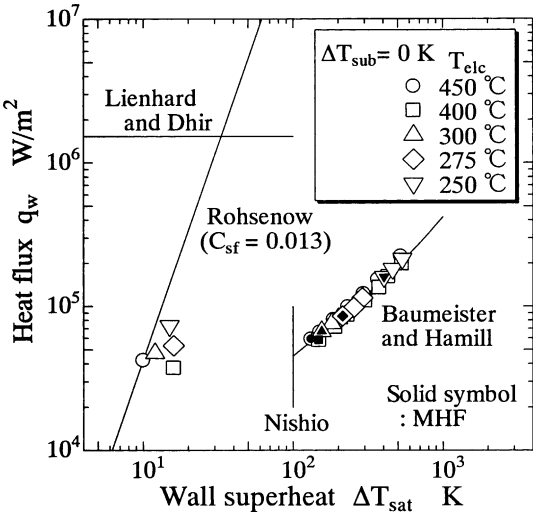

Fig. 4. Effect of local-cold spot temperature on boiling curve.

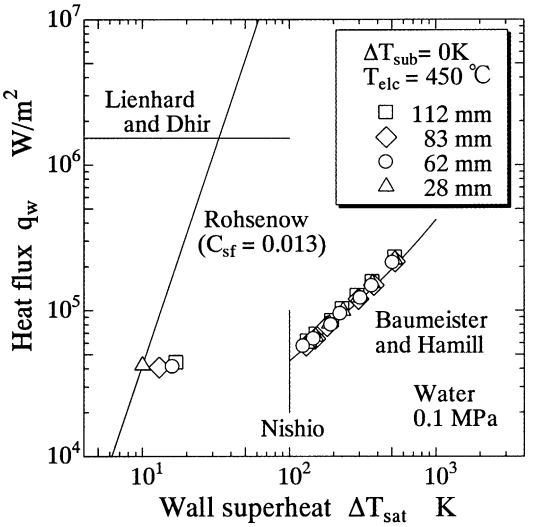

Fig. 3. Typical boiling curves.

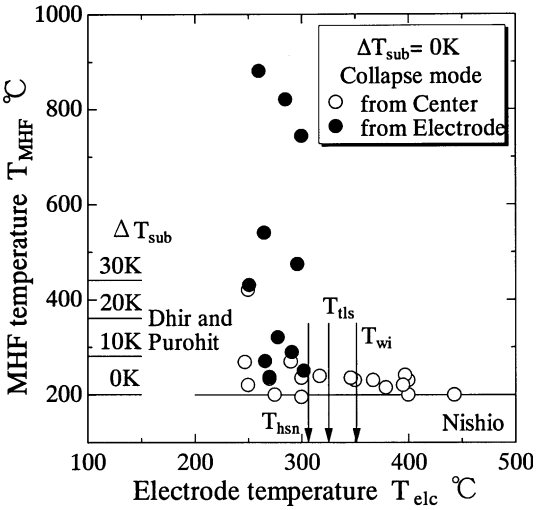

Fig. 5. MHF temperature at $\Delta T_{sub} = 0$ K.

of the electrode temperature. As seen from Fig. 5, the vapor film usually collapse at fairly high surface temperature when the temperature of the electrode is less than 300 °C, and T_{MHF} distribute widely from 200 to 900 °C independent of T_{elc}. In addition, as seen by the grouping of data points in the figure, we can see a systematic difference in the MHF-point temperature depending on the manner in which the vapor-film collapses; we could observe two types of vapor-film collapses in the present series of experiments under saturated boiling conditions. The two collapse types observed are as follows: independent of the electrode temperature, one type of collapse (open circles in Fig. 5) was that occurred around $T_{MHF} = 200$ °C in the central section of the heat transfer surface, spreading at a high propagation rate; the other type of collapse (solid circles in Fig. 5) was that started from the electrodes, spreading at relatively slow rate of propagation. In order to clarify the above classification of collapse types, we showed in Fig. 6 the relationship between the propagation velocity w of the collapse front of the vapor-film and MHF-point temperature; for the purpose of reference, shown in Fig. 6 are the propagation velocity measurements of Nishio et al. [6] for a 2 mm diameter platinum wire in water under one atmosphere. Also shown there are the numerical results of Dhir and Purohit relationship [4], Eq. (3), which is a generalized relationship for MHF-point temperature under subcooled boiling.

Fig. 6 shows that the experimental values of MHF-point temperature are such that they tend to become higher when the electrode temperature is reduced, even in the case of saturated boiling. It also shows that when the electrode temperature is high, the propagation velocity has become faster than 40 mm/s in the neighborhood of $T_{MHF} = 200$ °C. Another observation is that

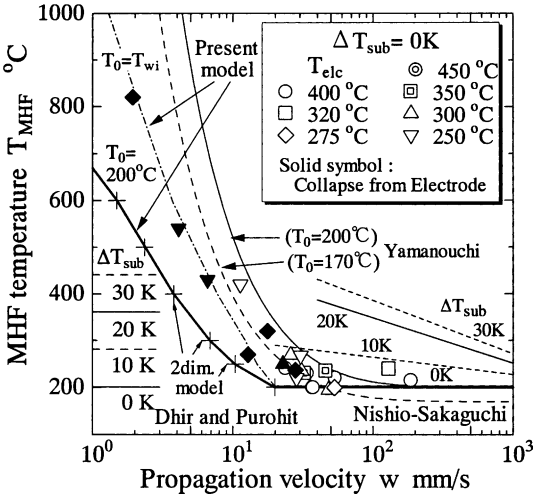

Fig. 6. Propagation velocity at $\Delta T_{sub} = 0$ K.

when the MHF-point temperature is increased, the propagation velocity becomes slow. This relationship between the MHF-point temperature and propagation velocity has the same trend as in the experimental evidence provided by Nishio et al. [6] for subcooled boiling. These two types of propagation can be thought to correspond with the coherent collapse (open circles in Fig. 5) and propagative collapse (solid circles in Fig. 5), which were mentioned in the introduction.

In the case of the latter, reducing the electrode temperature caused the MHF-point temperature to become elevated, and the propagation velocity to become slower. The MHF-point temperature became elevated and the MHF-point temperature became spread over a large temperature range, when the electrode temperature was reduced, as indicated in Fig. 5, especially below the thermodynamic limit of liquid superheat T_{tls} (by Lienhard [12]) for the liquid given by

$$(T_{tls} - T_{sat})/T_{cr} = 0.923 - (T_{sat}/T_{cr}) + 0.077(T_{sat}/T_{cr})^9, \tag{6}$$

$$T_{tls} = 325\ ^\circ\mathrm{C}, \tag{6'}$$

or more specifically, below the spontaneous homogeneous nucleation temperature T_{shn}

$$T_{shn} = 306\ ^\circ\mathrm{C} \tag{7'}$$

which was computed by using the spontaneous homogeneous nucleation rate [13] given by

$$J_{homo} = N\sqrt{\frac{2\sigma}{\pi m B}}\exp\left[-\frac{16\pi\sigma^3}{3k_B T_{hsn}(p_{ve}-p_l)^2}\right] \approx 10^6\ [\mathrm{cm^{-3}\,s^{-1}}]. \tag{7}$$

In the above equations, the following notations have been used: B is a constant ($=2/3$), J_{homo} is the nucleation rate at homogeneous state, k_B is Boltzmann constant ($=1.381\times10^{-23}$ J/K), m is mass of one molecule of liquid, N is number of molecules per unit volume of liquid, p is pressure, and T_{cr} is the critical temperature. In addition, the pressure p_{ve} of a spherical vapor bubble in equilibrium state is given by

$$p_{ve} = p_{sat}(T)\exp[-(v_l/k_B T)\{p_{sat}(T) - p_l\}], \tag{8}$$

where $p_{sat}(T)$ is the saturation pressure at temperature T and v_l is the volume occupied by one molecule of liquid ($=1/N$). Also note that T_{wi} of Fig. 5 is the maximum wall temperature that allows liquid–solid contacts to be made physically; namely, with reference to a two-body contact problem, T_{wi} is the initial temperature of the warmer body given by the following equation [14]

$$\frac{T_{wi} - T_{tls}}{T_{tls} - T_l} = \sqrt{\frac{(\rho c_p k)_l}{(\rho c_p k)_w}} \tag{9}$$

that makes the interface temperature the thermodynamic limit of liquid superheat when the two half-infinite bodies of different temperatures come into contact with each other; in Eq. (9), suffix w represents the wall. In conclusion, with reference to the experimental results of saturated boiling in which the weak spots in the central heat transfer section have been eliminated, we can say that localized collapse of film-boiling vapor film will take place from the low-temperature section, which is below the limit of superheat; we came to this conclusion based on the evidence that propagative type of vapor-film collapse occurred when the temperature of localized low-temperature section was below the thermodynamic limit of superheat (or spontaneous homogeneous nucleation temperature). We will explain the curves of Fig. 6 in the section to follow.

3.2. Subcooled boiling

Processing similar to Figs. 5 and 6, we show in Figs. 7 and 8 the case of $\Delta T_{sub} = 10$ K, and in Figs. 9 and 10 the case of $\Delta T_{sub} = 20$ K. Although Figs. 7 and 9 have rather irregular points (indicated by double circle symbols and hollow circle symbols respectively), they show trends similar to those found in the results of saturated boiling. Namely, when electrode temperature is below the superheat limit, the MHF-point temperature has become elevated and spread over a wide range of temperatures; the collapse of vapor-film occurred in two ways: one was the collapse that occurred in the middle of heat transfer surface and the other was that occurred at the electrodes. However, there are differences from the case of saturated-state boiling. Firstly, MHF-point temperature did not show a systematic change depending on the way the vapor-film collapsed. Secondly, even

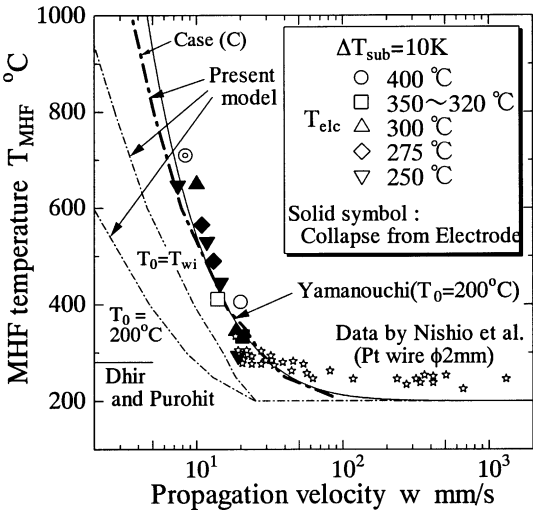

Fig. 8. Propagation velocity at $\Delta T_{sub} = 10$ K.

with respect to experiments where electrode temperatures were high, the collapse temperature of film-boiling vapor film was often higher than the value predicted by the equation of Dhir and Purohit, and was more than 100 °C higher than the thermodynamic limit of liquid superheat. Especially, the lower limit of MHF-point temperature obtained in the present experiments was not 200 °C; rather, it was close to the value given by Dhir and Purohit equation.

The above-mentioned trends of the MHF-point temperature to become warmer are very different from the experimental results reported by others [5–7] for systems, in which the weak-spot effect had been eliminated. Searching for an answer for this phenomenon

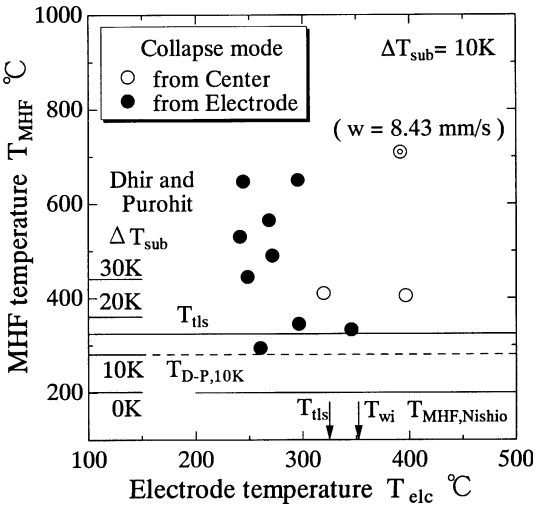

Fig. 7. MHF temperature at $\Delta T_{sub} = 10$ K.

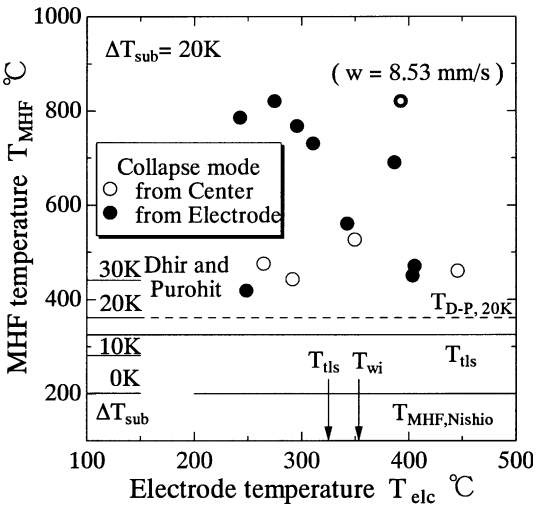

Fig. 9. MHF temperature at $\Delta T_{sub} = 20$ K.

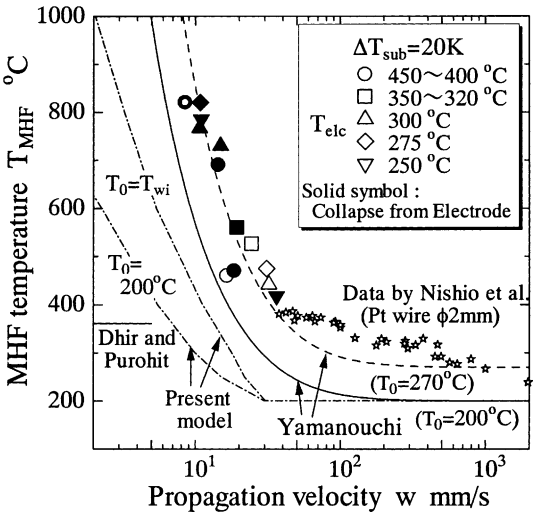

Fig. 10. Propagation velocity at $\Delta T_{sub} = 20$ K.

based on our observation results, we could observe in our subcooled-boiling experimental results that when the vapor film supposedly collapsed from the central section, it had actually started to collapse from the point where the voltage taps were welded to the heat transfer surface. Now, if we are to calculate a vapor-film thickness by simple heat conduction through the vapor film, the vapor-film thickness ($\delta_v = k_v/h_f$) will be approximately 80 μm for saturated boiling, 65 μm for subcooled boiling of 10 K liquid subcooling, and 55 μm for a 20 K subcooling. Namely, these thicknesses for subcooled boiling are comparable to the diameter of voltage taps. Therefore, it may be possible that the collapse of the vapor-film only appeared to have occurred in the central section in the present subcooled boiling experiments. In reality, however, the vapor-film collapse could have been a propagative type collapse started from the weak spot present at the weld-joint between the voltage tap and heat transfer surface. According to the previous numerical model by using transient heat conduction in a finite cylinder three-dimensionally and the boundary condition of the weak spot, the temperature drop at the welding spots is about 75 °C for the case of $T_w = 500$ °C and $\Delta T_{sub} = 20$ K; the drop is larger than that for the case of saturated boiling. Namely, it will be expected that there will exist a low-temperature section whose temperature is below the localized limit of liquid superheat (about 325 °C for water at atmospheric condition) if the wall temperature of the cylinder is about 400 °C and its cylinder has a weak spot whose dimension is 30 μm. In addition, in the experiments of high electrode temperatures, a propagative type vapor-film collapse was also observed to be occurring on the heat transfer surface from a place close to the electrodes as a result of the detachment of the vapor film at the electrodes. Examining Figs. 8 and 10, we can see that the relationship between the propagation velocity of vapor-film collapse and MHF-point temperature resembles that of saturated boiling experiments, and therefore, we can speculate that vapor collapse could have been a propagative type of collapse for most of subcooled boiling experiments in the present work. The following can be thought of as the main factors that will make the weld-joints of voltage-tap and the neighborhoods of high-temperature electrodes become weak spots in the case of subcooled boiling: the relationship between the voltage-tap size and film-boiling vapor-film thickness; and effects of heat capacity of the heat transfer surface when subcooled liquid comes into contact with the heat transfer surface. Especially, these factors had a significant effect on the experimental results of 20 K liquid subcooling, and the lower limit of MHF-point temperature of the present experiment was about 50 °C higher than the predicted value of Dhir and Purohit equation. As shown in Figs. 8 and 10, the experimental results of Nishio et al. [6] (for a 2 mm diameter platinum wire and 30 μm diameter voltage taps) lie on the extrapolation of the results of the present subcooled boiling experiments. If the heater will be clear of the weak spots completely, MHF-point temperature will decrease up to 100 °C gradually and propagation velocity of vapor-film collapse will be rapid increase with an increasing electrode temperature. On the other hand, in the case of saturated boiling experiments of the previous section, we expect the effects of the weak spots due to factors such as weld-joint of voltage taps to be less significant, because the film-boiling vapor-film thickness is sufficiently larger than the diameter of the voltage tap.

4. Modeling of vapor-film collapse and mechanism of vapor-film collapse at high wall temperature

4.1. Analytical model

Summarizing the above, we saw that the weak spot, namely the localized low-temperature section was closely related to the way in which the film-boiling vapor-film collapsed, and that this way of collapse affected the temperature of MHF point to a great extent. This localized low-temperature section corresponds to the support structures of heat transfer surfaces, in relating the present work to published works [5–7]. In industrial applications, we can expect the localized low-temperature regions to exist in various forms such as supports, protruded sections, and pointed segments. It has been suggested that effects of these factor would be important in assessing quench characteristics in practice. In the process of the propagative collapse of film-boiling vapor film, in addition to the heat transfer coefficient of the boiling surface, the heat conduction underneath the

boiling surface will also play a role. This vapor-film collapse process resembles [6] the rewetting process of a nuclear reactor rod; the rewetting occurs in a nuclear reactor when the emergent care cooling system is activated by the loss-of-coolant accident of the light-water-reactor. Therefore, we first attempted to make a quantitative investigation of the process of propagative collapse of a film-boiling vapor-film by using Yamauchi equation [15], which represents rewetting under a falling-flow of a liquid layer:

$$w = (1/\rho_w c_w)\sqrt{hk_w/\delta_w}(T_0 - T_s)/\sqrt{(T_w - T_0)(T_w - T_s)}. \quad (10)$$

In this attempt, we made the following assumptions, which are also depicted in Fig. 11: (1) T_{MHF}, namely the average temperature of heat transfer surface in the instance of vapor-film collapse was equal to dried-out surface temperature T_w. (2) Temperature at collapse-front T_0 was considered to be 200 °C, which is the true MHF-point temperature under idealized conditions. (3) Typical heat transfer coefficient on the wetted-side was given by the critical heat-flux conditions as specified by equations for q_{nb} [9] and q_{CHF} [10], namely: $h_l = q_{CHF,sat}/\Delta T_{CHF,sat} = 1.31/31.5$ MW/m^2 K at $\Delta T_{sub} = 0$ K, $h_l = q_{CHF,sub10}/(T_{CHF,10} - T_{l,10}) = 1.93/45.9$ MW/m^2 K at $\Delta T_{sub} = 10$ K and $h_l = q_{CHF,sub20}/(T_{CHF,20} - T_{l,20}) = 2.55/59.4$ MW/m^2 K at $\Delta T_{sub} = 20$ K. (4) Heat transfer coefficient on the dried-out side was neglected. (5) Wetted-side temperature T_s was set to liquid temperature T_l.

In addition, in conformity with the heat conduction equation in cylindrical coordinates system, we gave the typical dimension to be $\delta_w = d/4$, where d is the wire diameter. Note also that this model did not take into account Joule heat generation.

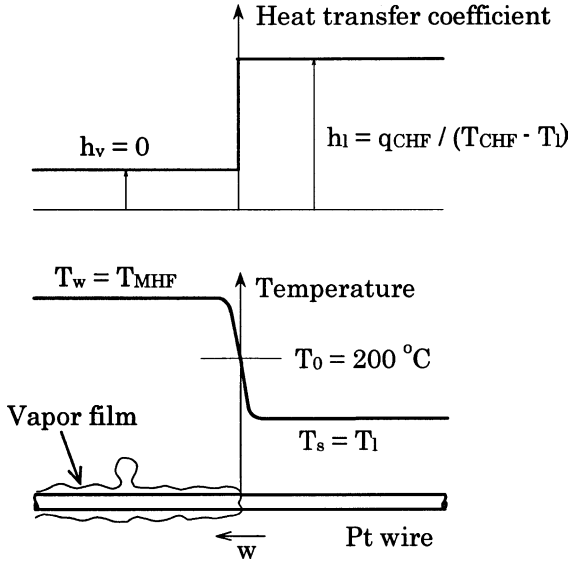

Fig. 11. Application of Yamanouchi's model.

If we now display the numerical results from the above model calculations as trends of T_{MHF} in Figs. 6, 8 and 10, we can see that the results are in good agreement with the present experimental results qualitatively. However, concerning quantitative agreement, we can see that there are slight discrepancies between the numerical and experimental results in the cases of liquid subcoolings, $\Delta T_{sub} = 0$ K and $\Delta T_{sub} = 20$ K. Apart from these discrepancies, we can see that the propagative collapse of vapor-film in film boiling shows the same characteristics as the rewetting process. As mentioned the previous section, the results of the present subcooled boiling experiments lie on the extrapolation of the experimental results of Nishio et al. [6] (for a 2 mm diameter platinum wire), if the extrapolation is based on the trend predicted by the present model simulations. This agreement shows that the present experimental results of subcooled boiling represent propagative type of collapse from weak spots.

For further investigation, we shall now attempt a simplified simulation of the process by focusing on the collapse-front temperature T_0. If we seek a value for T_0 that will best fit the present experimental results assuming the previous assumptions (1), (3), (4) and (5) to hold, we get the following results, which are shown in Figs. 6, 8 and 10: for $\Delta T_{sub} = 0$ K, $T_{0,sat} = 170$ °C; for $\Delta T_{sub} = 10$ K, $T_{0,sub10} = 200$ °C and for $\Delta T_{sub} = 20$ K, $T_{0,sub20} = 270$ °C. Note that all these temperatures are below the limit of liquid superheat, and it suggests that the vapor-film collapse-front temperature T_0 will be below the temperature of superheat limit, even if the overall average temperature of the heat transfer surface at the moment of vapor-film collapse is higher than the temperature at the limit of superheat; note that T_0 is the temperature of the section where liquid–solid contact occurs.

4.2. Numerical simulation

In the previous analytical model, we have neglected some effects on the propagation velocity of vapor-film collapse by the assumptions of the model. For instance, the assumption that the heat transfer coefficient in the wetted section is fixed at CHF condition will overestimate the collapse velocity. Similarly, the assumption that Joule heating in the heat transfer surface is negligible, will overestimate the collapse velocity because heat recovery is only heat conductive effect. The assumption that the heat transfer coefficient in the dry-out section is negligible will underestimate the collapse velocity. To address these issues, we will attempt to develop the present analytical model into a much more advanced model by using numerical analysis. In this model, we will attempt to address the mechanism of vapor-film collapse also.

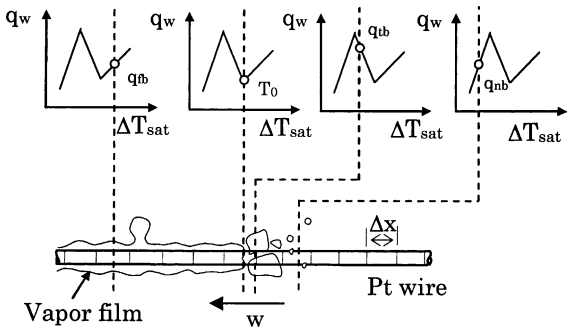

Fig. 12. Numerical model of vapor-film collapse.

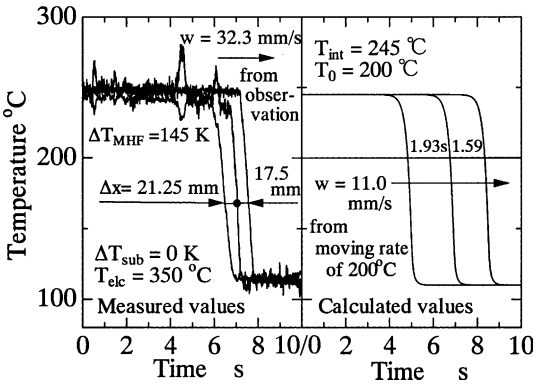

Fig. 13. Comparison with measured cooling curves and calculated values.

As in Ref. [16], to model the vapor-film collapse process, we consider a finite cylinder as shown in Fig. 12 and analyze transient heat conduction in it one-dimensionally by using the following equation:

$$\rho c\frac{T_i^{k+1}-T_i^k}{\Delta t}=k\frac{T_{i+1}^k-2T_i^k+T_{i-1}^k}{\Delta x^2}-\frac{h\Delta T_{\mathrm{sat}}\pi D}{(\pi/4)D^2}+\rho_{\mathrm{e}}\frac{I^2}{(\pi/4\cdot D^2)^2}. \tag{11}$$

We will use the pool boiling heat transfer characteristics as the boundary condition of the heat transfer surface. The heat transfer characteristics on the boundary conditions are as follows: (a) the heat flux q_{fb} in the dry-out area is the Baumeister and Hamil's equation for the coefficient of film-boiling heat transfer around a horizontal cylinder under natural convection, (b) film-boiling collapse-front temperature T_0 is Nishio's equation for MHF-point temperature under idealized conditions, (c) the heat flux q_{tb} soon after the surface gets wet is given by a straight line on the boiling curve; one end of the line is the point of film-boiling heat flux q_0 that corresponds to the vapor-film collapse temperature T_0 and the other is the point of q_{CHF} obtained from Lienhard and Dhir's equation for the critical heat flux of a horizontal cylinder, (d) the heat flux q_{nb} in other wetted areas is the value computed from Rohsenow's empirical equation for nucleate boiling heat transfer. When considering the effects of Joule heat generation, we took into account temperature dependence of electrical resistance of the wire in the present model. However, in order to model the collapse of the vapor film, we have made one end of the wire a singular point by assigning it both the temperature T_{wi} (Eq. (9)) that is the maximum wetting temperature and the critical heat flux q_{CHF}. This assignment was done in order to model the electrodes and liquid–solid contacts at heat transfer surface due to the liquid invasion [6]; the latter occurs when a vapor dome is detached as a result of Rayleigh–Taylor instability.

A sample calculation using the above model is shown in Fig. 13. The left-hand section of Fig. 13 shows our experiment results for the cooling curves in the vapor-film collapse process recorded using the A/D port. Each interval between voltage taps is 27.5, 15 and 20 mm: the interval between the middle of the measurement segment of wire between a pair of voltage taps is 21.25 and 17.5 mm, respectively. As shown in Fig. 13 we have obtained a cooling characteristic that is in qualitative agreement with the experiments. However, we can observe a quantitative difference between the measured collapse velocity (32.3 mm/s) of vapor film that was based on observations, and the computed velocity (11.0 mm/s), which is derived from the difference of the time of MHF point ($T_{\mathrm{w}} = 200$ °C) and the distance between neighboring calculative locations. In the present work, based on Ref. [16], we expected that the collapse velocity of vapor film would correspond with the translation velocity of T_0 point: T_0 corresponds with the MHF point on a pseudo boiling curve at the point. We shall try to compare the numerical and experimental results in this regard.

In Fig. 6, we have shown numerical results with for a strong solid-line the initial overall average temperature of the heat transfer surface, namely T_{MHF} obtained from the present numerical simulations for saturated boiling condition. Fig. 6 shows that the present numerical simulations underestimate the collapse velocity of film-boiling vapor film: this is clear by comparing the translation velocity of T_0, which is output of the model and the present experimental results on the collapse velocity. However, the trends of the simulation are in good agreement with those of the experiments. We have also shown with a chain-line in Fig. 6 the results of the simulation in which we assumed that the boundary condition shown in Fig. 14, namely the temperature of vapor-film collapse (MHF-point temperature of pseudo

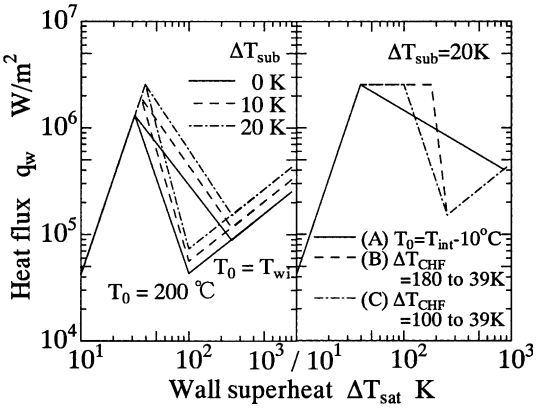

Fig. 14. Postulated boiling curves.

boiling curve) was the condition of the maximum wall temperature for physical liquid–solid contacts to occur, namely

$$T_0 = T_{\mathrm{wi}}, \tag{12}$$

where T_{wi} was obtained from Eq. (9). As seen from Fig. 6, these results describe well the experimental results both qualitatively and quantitatively. Although a further detailed analysis will require an accurate relationship for the transition-boiling region, the results of Fig. 6 show that the temperature at which the film-boiling vapor-film collapses cannot exceed T_{wi}, which is the maximum contact-temperature based on the thermodynamic limit of liquid superheat.

In order to confirm an effect of radial component in heat conduction on the above model, we also calculate transient heat conduction in a finite cylinder two-dimensionally. From the present simulations, a typical different between wall and center of the cylinder temperatures on film boiling is about 1 K; the temperature different between the wall and the center at just the condition for physical liquid–solid contacts is about 5 K. The results of calculation using the two-dimensional model have been shown in Fig. 6. As seen from Fig. 6, the results coincide with those by the one-dimensional model. Therefore, the present numerical model depends little upon the radial heat conduction. A typical Biot number in film-boiling regime is about 0.05.

Figs. 8 and 10 show the results of numerical simulations of similar nature obtained for subcooled boiling. In these calculations, in order to account for the effects of liquid subcooling, we used the CHF given by [17]:

$$q_{\mathrm{CHF,sub}} = q_{\mathrm{CHF,sat}}[1 + 0.1(\rho_{\mathrm{v}}/\rho_{\mathrm{l}})^{0.25} \times (\rho_{\mathrm{l}} c_{pl} \Delta T_{\mathrm{sub}}/\rho_{\mathrm{v}} h_{\mathrm{fg}})], \tag{13}$$

and film-boiling heat transfer rates given by

$$h_{\mathrm{f,sub10}}/h_{\mathrm{f,sat}} = 1.3, \tag{14}$$

$$h_{\mathrm{f,sub20}}/h_{\mathrm{f,sat}} = 1.7, \tag{15}$$

which are the results of two-phase boundary-layer theory [18] evaluated for present system. Figs. 8 and 10 show that numerical results are in good agreement with the experimental results qualitatively. Comparing the figures, we can also see that even the numerical simulations that assume the maximum physical contact temperature to be given by Eq. (12) have underestimated the experimental results when the liquid subcooling was increased.

To examine the above quantitative differences in the results for subcooled conditions, we attempted a numerical experiment, in which we varied the boiling curve of Fig. 14, especially the characteristics of the transition portion of the curve, which was used in the boundary condition. We used two cases of computations: In case A, the vapor-film collapse temperature T_0 can have a temperature higher than the limit of liquid superheat:

$$T_0 = \text{initial wall temperature} - 10\ ^{\circ}\mathrm{C}. \tag{16}$$

Here the initial wall temperature is wall temperature during stable film-boiling state; the temperature is a calculative parameter. In case B, the vapor-film collapse temperature T_0 was restricted to the maximum contact-temperature based on the limit of superheat; and in addition, the heat flux in the transition-boiling region was raised. Namely, in addition to $T_0 = T_i$, we varied the values assigned to the upper limit of the superheat for the critical heat-flux region as given below:

$$\Delta T_{\mathrm{CHF}} = 180 \text{ to } 39.4 \text{ K} \quad \text{for} \quad \Delta T_{\mathrm{sub}} = 20 \text{ K}. \tag{17}$$

Computations for both the cases A and B were carried out at $\Delta T_{\mathrm{sub}} = 20$ K, and their results compared with experimental results in Fig. 15. The experimental results

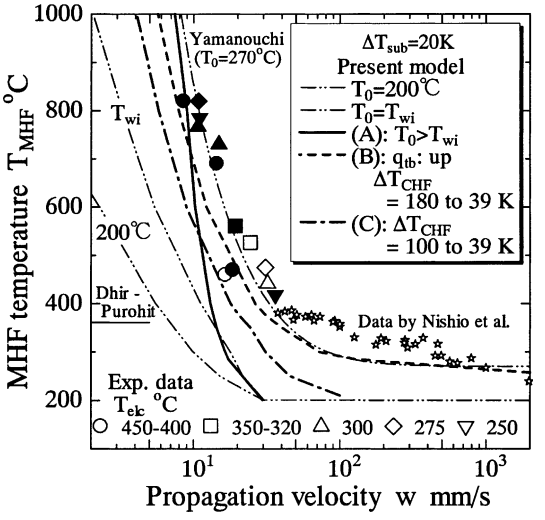

Fig. 15. Results of numerical simulations.

for low MHF-point temperatures are few in number; note that T_{MHF} is the average temperature of heat transfer surface at the instance of vapor-film collapse. Fig. 15 makes it clear that the results of case B in which we raised the heat flux in the transition-boiling region, can describe the experimental results well, both qualitatively and quantitatively more than it does by the case A in which we assumed a vapor-film collapse temperature T_0 that was higher than the thermodynamic limit of liquid superheat. To pursue this work further, it will be necessary to have an accurate relationship for heat transfer in the transition boiling region as previously stated. However, the present results suggest that the temperature T_0 of vapor-film collapse-front cannot exceed T_{wi} even in the case of subcooled boiling, a known fact for saturated boiling as stated previously; note that T_0 is the temperature of liquid–solid contacts section and T_{wi} is the maximum contact-temperature based on the limit of liquid superheat.

According to published experimental evidence [19] on transition-boiling heat transfer, boiling curve in the transition region has a upward-convex shape, which is closer to case B than to case A. For the purpose of reference, we also perform the computations for the case C in which the upper limit of degree of superheat of the critical heat-flux region was set to 100 K, because both situations for the cases A and B are very far from the ordinary boiling curve. We have also shown in Fig. 8 for $\Delta T_{sub} = 10$ K and Fig. 14 for $\Delta T_{sub} = 20$ K by thick chain-lines the numerical results of the case C; the boiling curve is more realistic in terms of heat transfer characteristics (see Fig. 14).

In summary, for the process of propagative collapse of a vapor-film, we confirmed that heat conduction within the heat transfer surface would act as one of the major governing factors in addition to thermo-fluid conditions for film boiling. In addition, the present work suggests that localized temperature of the collapse front of vapor-film T_0 will not exceed the temperature of thermodynamic limit of liquid superheat T_{tls}. In other words, if there exists a low-temperature section whose temperature is below the localized limit of liquid superheat (more accurately, the spontaneous homogenous nucleation temperature T_{shn} or the maximum contact temperature T_{wi} that corresponds to T_{shn}), then the vapor film will collapse locally from this location, even if the heat transfer surface, as a whole is maintained at an average temperature above the T_{tls}. The surroundings of the local spot will be cooled by heat conduction through the solid, and the collapse of vapor-film will propagate to other areas from the local point. However, the temperature T_0 of liquid–solid contacts section cannot exceed the maximum contact temperature T_{wi}, which results from the T_{tls}. This explanation can be considered as the mechanism of MHF-point temperature that is encountered in industrial applications. This explanation is also consistent both quantitatively and physically in that MHF-point temperature can exceed the T_{tls}.

5. Conclusions

This paper reports results of a study conducted to examine effects of the temperature of a localized low-temperature region on the followings: film-boiling vapor-film collapse condition represented by MHF-point temperature for a heated surface of high superheat, the way in which vapor-film collapses, and the vapor-film collapse velocity. Conclusions of this study are as follows:

1. When the temperature of low-temperature section decreases, the MHF-point temperature (namely, the average temperature of heat transfer surface at the instance of vapor-film collapse) gets elevated; conversely, the propagation velocity of vapor-film collapse decreases. The MHF point gets rapidly elevated in temperature particularly when the low-temperature section has a lower temperature than that at the thermodynamic limit of liquid superheat (more accurately, spontaneous homogeneous nucleation temperature); the propagation velocity also gets slower in this case.
2. Characteristics of propagative vapor-film collapse can be described by a model, in which heat conduction is considered and known empirical relationships for boiling heat transfer used. In addition, this model showed that the temperature of the vapor-film collapse-front could not exceed the maximum contact temperature, which was obtained by considering the thermodynamic limit of liquid superheat and two-body contact model.
3. Above (1) and (2) portray a phenomenon, which can be described as follows: if a localized low-temperature section exits, and if its temperature is below the localized limit of liquid superheat (more accurately, the spontaneous homogeneous nucleation temperature), then the vapor-film will collapse at this point even if the heat transfer surface is maintained as a whole at an average temperature, which is above the temperature at the thermodynamic limit of liquid superheat. The collapse point will then propagate to other areas by way of cooling its surroundings by heat conduction through the body of the heat transfer surface. However, the temperature of liquid–solid contact section cannot exceed the maximum contact-temperature based on the thermodynamic limit of liquid superheat.
4. Considering the above process to represent the mechanism of MHF-point temperature encountered in industrial applications, we proposed one solution to explain the fact that MHF-point temperature can ex-

ceed the temperature at thermodynamic limit of liquid superheat; this solution was consistent both quantitatively and physically.

Acknowledgements

The authors gratefully acknowledge the support for this study by the research fund (Grant-in-Aid for Encouragement of Young Scientists, No. 06750215, and Grant-in Aid for Scientific Research (c), No. 09650254) of the Ministry of Education, Culture, Sports, Science and Technology of Japan. They are indebted to Prof. Tatsuhiro Ueda for many helpful and stimulating discussions for this work.

References

[1] S. Nukiyama, The maximum and minimum values of the heat Q transmitted from metal to boiling water under atmospheric pressure, J. Soc. Mech. Engrs. (Jpn.) 37 (1934) 367–374.
[2] P.J. Berenson, Film-boiling heat transfer from a horizontal surface, Trans. ASME, J. Heat Transfer 83 (1961) 351–358.
[3] S. Nishio, Prediction technique for minimum-heat-flux (MHF)-point condition of saturated pool boiling, Int. J. Heat Mass Transfer 30 (1987) 2045–2057.
[4] V.K. Dhir, G.P. Purohit, Subcooled film-boiling heat transfer from spheres, Nucl. Eng. Des. 47 (1978) 49–66.
[5] M. Narazaki, S. Fuchizawa, M. Usuba, Effects of specimen geometry on characteristic temperature during quenching of heated metals in subcooled water, Tetsu Hagane (Jpn.) 75 (1989) 64–71.
[6] S. Nishio, M. Uemura, K. Sakaguchi, Film boiling heat transfer and minimum-heat-flux-point condition in subcooled pool boiling, JSME Int. J. (Ser. II) 30 (1987) 1274–1281.
[7] Y. Kikuchi, M. Nagase, I. Michiyoshi, On the low limit of subcooled film boiling, Trans. JSME, (Jpn.) Ser. B 54 (1988) 2830–2837.
[8] Japanese Industrial Standard C 1604, 1989.
[9] W.M. Rohsenow, A method of correlating heat-transfer data for surface boiling of liquids, Trans. ASME, J. Heat Transfer 74 (1952) 969–975.
[10] J.H. Lienhard, V.K. Dhir, Hydrodynamic prediction of peak pool-boiling heat fluxes from finite bodies, Trans. ASME, J. Heat Transfer 95 (1973) 152–158.
[11] K.J. Baumeister, T.D. Hamill, Laminar flow analysis of film boiling from a horizontal wire, NASA TN D-4035, 1967.
[12] J.H. Lienhard, The properties and behavior of superheated liquids, Lat. Am. J. Heat Mass Transfer 10 (1986) 169–187.
[13] V.P. Carey, Liquid–vapor phase-change phenomena, Hemisphere Publishing Corporation, 1992, p. 149.
[14] S.-C. Yao, R.E. Henry, An investigation of the minimum film boiling temperature on horizontal surfaces, Trans. ASME, J. Heat Transfer 100 (1978) 260–267.
[15] A. Yamanouchi, Effect of core spray cooling in transient state after loss of coolant accident, J. Nucl. Sci. Technol. 5 (1968) 547–558.
[16] H. Ohtake, Y. Koizumi, Study on rewetting of vertical-hot-thick surface by a falling film (investigation from the aspect of boiling heat transfer characteristics and modeling), in: 11th Int. Heat Transfer Conf., vol. 2, 1988, pp. 325–330.
[17] H.J. Ivey, D.J. Morris, Rept. AEEWR 137, UKAEA, Winfrith (1962)—referring from ibid [13].
[18] S. Nishio, H. Ohtake, Vapor-film-unit model and heat transfer correlation for natural-convection film boiling with wave motion under subcooled conditions, Int. J. Heat Mass Transfer 36 (1993) 2541–2552.
[19] T.D. Bui, V.K. Dhir, Transition boiling heat transfer on a vertical surface, Trans. ASME, J. Heat Transfer 107 (1985) 756–763.